ELSEVIER

Biochimica et Biophysica Acta 1237 (1995) 135–142

BBA Biochimica et Biophysica Acta

Phase behaviour of distearoylphosphatidylethanolamine in glycerol – a thermal and X-ray diffraction study

Zhi-Wu Yu [a], Nelly M. Tsvetkova [b], Latchezar I. Tsonev [c], Peter J. Quinn [a,*]

[a] *Division of Life Sciences, King's College London, Campden Hill Road, London, W8 7AH, UK*
[b] *Central Laboratory of Biophysics, Bulgarian Academy of Sciences, Sofia, Bulgaria*
[c] *Institute of Cryobiology and Freeze-drying, Sofia, Bulgaria*

Received 1 December 1994; revised 7 March 1995; accepted 30 March 1995

Abstract

The phase behaviour of 1,2-distearoylphosphatidylethanolamine in glycerol has been examined using differential scanning calorimetry and real-time synchrotron X-ray diffraction methods. Dry phospholipid and phospholipid dispersed in glycerol over the concentration range 2.4%–90% (w/w) was equilibrated for 30 min at 20° C and thermal and structural parameters on the temperature range 60° C to 110° C recorded during an initial heating and subsequent reheating. The characteristic feature of the initial heating scan was a direct lamellar crystalline to inverted hexagonal phase transition. In the subsequent cooling scan a lamellar gel structure was formed from the non-lamellar phase which transformed, on reheating, to a lamellar crystalline phase in which the acyl chain packing was tilted with respect to the bilayer plane. The mechanism of the formation of the two crystalline phases was examined in the context of a relaxation model, where the liquid-crystal phase below the transition temperature from lamellar crystalline phase is metastable. A binary phase diagram over the temperature range 60° C to 110° C has been constructed.

Keywords: Glycerol; Phosphatidylethanolamine; Phase diagram; Phase behaviour; Crystallization; Cryoprotectant

1. Introduction

Continued efforts have been made to explore the molecular mechanisms whereby cryoprotective agents such as glycerol protect living organisms and tissues from cryoinjury [1–3]. It is generally believed that an important site of action of cryoprotectants is the membranes of cells where they appear to preserve the stability of these structures during either exposure to low temperature or upon recovery to the growth temperature. It was originally suggested that cryoprotective agents act to stabilize the membranes by preserving the lipid bilayer structure at low temperature [4,5]. Examination of the effect of a wide range of cryoprotective agents including disaccharides, sugar alcohols and polyols [6] and dimethyl sulfoxide [7] on the phase behaviour of model membrane systems show that liquid-crystal bilayer arrangements of phospholipids are in fact destabilized in favour of nonlamellar arrangements. This suggests that cryoprotective mechanisms may be more complicated than hitherto thought and are likely to be related to phase separation processes that are a consequence of exposure of complex biomembranes to temperatures that result in cryoinjury. To obtain a more complete understanding of the effect of cryoprotectants on multicomponent biomembrane systems, it is necessary to examine the effect of cryoprotectants on the phase behaviour of individual lipid classes which are represented in biological membranes.

Unlike the phase behaviour of small molecules, where equilibrium can be readily established, hysteresis and noncooperativity are common features of phase transitions in phospholipids [8]. For aqueous dispersions of phosphatidylethanolamines, a thermotropic phase transition sequence of lamellar-gel (L_β) → lamellar liquid-crystal (L_α) → inverted hexagonal (H_{II}) is normally observed during heating. However, other parameters like thermal history, concentration of cosolute/cosolvent, and extent of hydration are also important and some phase or phases may be

Abbreviations: DLPE, DMPE, DPPE, DSPE, DAPE, 1,2-dilauroyl-, dimyristoyl-, dipalmitoyl-, distearoyl-, and diarachidoylphosphatidylethanolamine; MGDG, monogalactosyldiacylglycerol; L_c and $L_{c'}$, normal and tilted lamellar crystalline phase; L_β, lamellar gel phase; H_{II}, inverted hexagonal phase.

* Corresponding author. Fax: +44 171 3334500.

SSDI 0005-2736(95)00097-6

omitted, other phases such as lamellar crystalline phases may form, or in some cases the phase sequence may be reversed. Although a considerable body of data concerning these properties of lipids in aqueous dispersions has become available during the last few decades, much less attention has been paid to the effect of nonaqueous solvents.

It is known that nonaqueous solvents induce unusual phases in membrane lipid analogues such as interdigitated lamellar phases [9,10] and non-lamellar phases where none exist in aqueous systems [11,12]. These effects are believed to result from changes in the interactive forces between the phospholipid molecules manifest as a change in surface area occupied by the polar group of the molecule at the solvent interface. There is as yet no correlation established between any easily characterised property of the solvent and structural alterations in the lipid phase.

Some studies have been reported on the effects of glycerol on the phase behaviour of the bilayer-forming lipid dipalmitoylphosphatidylcholine [13]. Our group has also examined the effect of aqueous glycerol solvent on the phase behaviour of the non-lamellar forming lipid, distearoylphosphatidylethanolamine [14]. It was found that increasing mole fractions of glycerol in water leads to a marked stabilization of lamellar crystal and hexagonal phases of the phospholipid. In the present study we have used differential scanning calorimetry and synchrotron X-ray diffraction methods to characterise the phase behaviour of distearoylphosphatidylethanolamine in glycerol and the data has been used to construct a binary phase diagram of the two components over the temperature range 70–110° C.

2. Materials and methods

Synthetic distearoylphosphatidylethanolamine (DSPE) and glycerol were purchased from Fluka AG; the lipid was found to be at least 99% pure by thin-layer chromatography. DSPE/glycerol mixtures were prepared by weighing. Samples were then equilibrated at 80° C for approx. 7 h and vortex mixed several times during the incubation. The composition of the binary system ranged from anhydrous DSPE to a dispersion with 90% by wt. of glycerol.

Thermal behaviour of the samples were examined using a DuPont 1090 thermal analyser. Phase transitions were recorded over the temperature range 20–135° C at a rate of 2 C°/min. To take account of the possibility of thermal decomposition of the lipid, transitions at temperatures greater than 100° C were invariably recorded on parallel samples in which one sample was stored below 100° C.

X-ray diffraction experiments were performed at station 8.2 of the Daresbury Synchrotron Radiation Source, UK, as previously described [15]. Calibration of the spacings was obtained by locating the beam centre by extrapolating four orders of a lamellar repeat spacing and the Bragg spacing of teflon [16].

3. Results

The phase behaviour of DSPE, in common with many phospholipids, exhibits pronounced hysteresis and it is convenient to consider the phase properties in samples equilibrated at temperatures where crystal phases form and those where metastable phases are likely to exist.

3.1. Thermally equilibrated dispersions

The thermal properties of DSPE dispersed in different weight percent ratios with glycerol were examined in samples that had been incubated for 7 h at 80° C and then equilibrated at 20° C for 30 min. The resulting DSC traces are presented in Fig. 1 (left). Dry DSPE shows a single endothermic phase transition centred at about 105° C. The

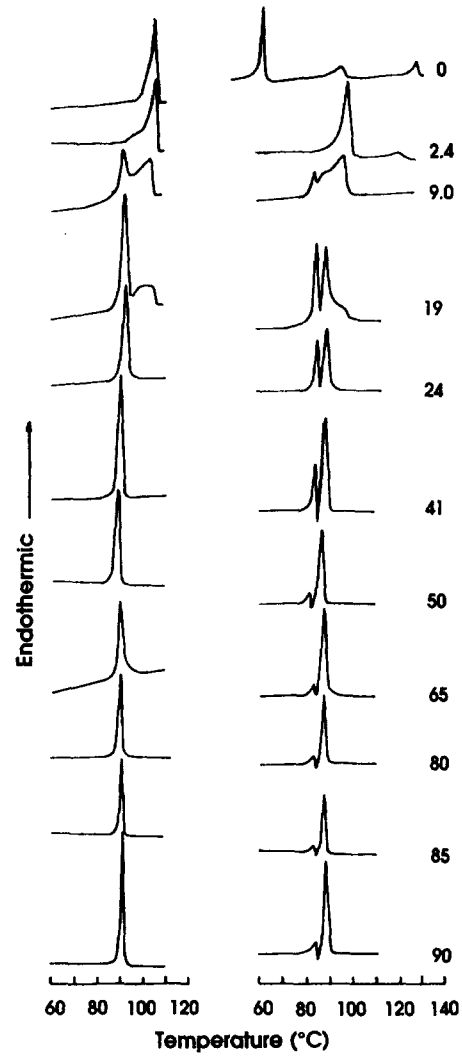

Fig. 1. Differential scanning calorimetric heating scans of distearoylphosphatidylethanolamine in glycerol with different solvent contents (w/w). Thermograms on the left were recorded during an initial heating of samples equilibrated for 30 min at 20° C, and thermograms on the right during reheating immediately after cooling from the liquid-crystal phase to 60° C (scanning rate 2 C° /min).

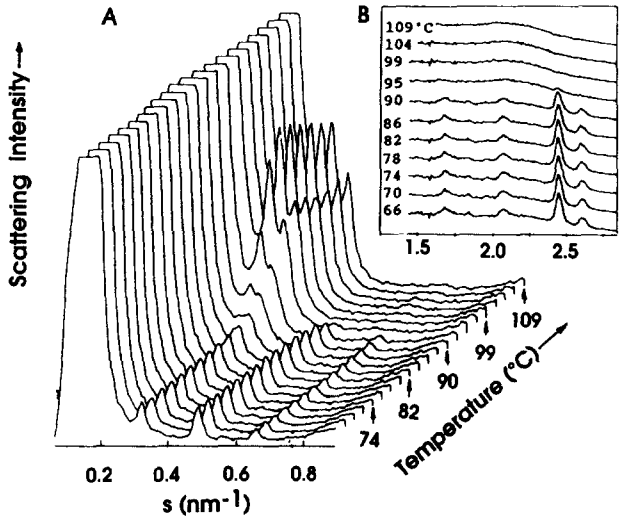

Fig. 2. Real-time X-ray diffraction patterns of distearoylphosphatidylethanolamine in glycerol (50%, w/w) showing lamellar-crystalline to inverted hexagonal phase transition. Data were obtained during an initial heating scan at 5 C°/min of a sample prepared as in Fig. 1. Each pattern represents scattering intensity accumulated during 24 s. (A) Small-angle scattering region; first order maxima are truncated to emphasize higher order diffractions; (B) corresponding wide-angle pattern scattering intensity.

addition of glycerol induces a new endothermic transition at 91.7° C and this completely replaces the high temperature transition when the solvent content reaches 24% (w/w) glycerol. Further increase in the concentration of glycerol slightly decreased the transition temperature but increased the cooperativity of the transition as evidenced by a sharpening of the endothermic peak. It is well known that an increase of the hydration water can reduce the acyl chain melting temperature of lipid mesophases and it appears that glycerol may act in a similar manner to water in this respect. The apparent two-transition feature at concentrations of glycerol between 9.0% and 19% (w/w) could be explained by some inhomogeneity of these samples. Strenuous attempts to achieve thorough mixing of the components did not affect the thermal behaviour shown at these low weight percentages of glycerol.

The identity of the phase structures before and after the transition observed with DSC was established by X-ray diffraction analysis. Typical real-time X-ray diffraction patterns recorded for a thermally-equilibrated sample of DSPE dispersed in 50% (w/w) glycerol during initial heating are presented in Fig. 2. This shows a phase transition from L_c to H_{II} at a temperature of 90° C. The L_c phase is characterized by the first four orders of diffraction indexing a *d*-spacing ratio 1:1/2:1/3:1/4 in the small-angle region (Fig. 2a) with two sharp diffractions and at least two less-prominent diffractions in the wide-angle region (Fig. 2b). The lamellar repeat spacing at 64° C is 6.07 nm and there is no significant change of this spacing up to about 86° C above which a new structure appears. The value for the lamellar repeat spacing is in good agreement with that of 6.1 nm at 60° C reported by Williams et al. [14] and a derived value of 6.0 nm from data reported by Seddon et al. [17]. The values of the two sharp wide-angle diffractions, 0.381 and 0.407 nm, and that of the two weak bands at 0.480 and 0.597 nm, respectively, are also in agreement with the respective values reported by Williams et al. [14]: 0.395, 0.370, 0.46 and 0.58 nm for the same lipid in glycerol (75%, w/w) at 60° C.

At temperatures greater than 89° C the X-ray diffraction maxima of the same dispersion exhibits a *d*-spacing ratio of $1:1/\sqrt{3}:1/\sqrt{4}$. In the wide-angle region, the sharp Bragg reflections of the L_c phase are replaced by a broad diffraction band, indicating disordered arrangement of the acyl chains of the lipid molecules. The band is centred at a position indicating a spacing of about 0.48 nm. This structure is consistent with an inverted hexagonal phase, or H_{II}.

Phase identification in the absence of glycerol or at low solvent concentrations, i.e., less than 24% (w/w) glycerol, is still problematic. Although the same lamellar phase (L_c) can be identified at temperatures less than ca. 90° C in the initial heating scan, another phase, which progressively replaces the L_c on heating, cannot be assigned unambiguously and may consist of a mixture of different phase structures. At temperatures greater than 90° C, the structure is usually characterised by a prominent first-order X-ray diffraction maximum, and occasionally weak higher-order diffractions can be detected at a position approx. $1/\sqrt{2}$ or $1/\sqrt{3}$ of the first-order repeat distance. This phase could be interpreted as a distorted lamellar phase which is unable to transform into an inverted hexagonal phase due to the lack of solvation of the polar group. We designate this phase α. The repeat distance of the α phase is between 3.58 and 3.77 nm, which is considerably less than that of the normal hexagonal phase formed in the presence of glycerol concentrations greater than 24% (w/w). Considering the fact that inverted hexagonal or micelle structures require a solvent core, such behaviour is not unexpected.

The relative intensities of the second and third order diffractions of both the lamellar and non-lamellar phases of DSPE decrease with decreasing glycerol concentration. This may suggest a gradual loss of long-range order in the repeat structures as discussed by Laggner [18].

3.2. Characterisation of metastable phases

Upon cooling from 110° C the apparent two-transition feature was again observed by differential scanning calorimetry at glycerol concentrations less than 24% (w/w), indicating that any inhomogeneous solvent distribution was not reversed by transformation into the liquid-crystal phase. With glycerol contents greater than 24% (w/w), exothermic phase transitions were recorded at temperatures about 16° C correspondingly lower than that observed during the initial heating scan (data not shown). X-ray diffraction patterns recorded during cooling scans

demonstrated that these transitions were from H_{II} phase directly to a lamellar-gel phase (L_{β}), characterised by a single sharp diffraction maximum around 0.42 nm in the wide-angle scattering region and a 1:1/2:1/3 *d*-spacing ratio in the small-angle scattering region. There was no evidence of any intermediate lamellar liquid-crystal phase in the phase transition sequence.

The complexity of the phase transition sequence was evident during a second heating scan conducted immediately following the cooling scan. These thermograms are presented in Fig. 1 (right).

Firstly, at least two endothermic phase transitions were observed in dry DSPE. Studies of related anhydrous lipids such as dilauroyl, dimyristoyl, and diarachidoyl derivatives of phosphatidylethanolamine [17] showed the existence of a, so-called, B phase abridging the L_c and H_{II} phases. The B phase was characterized in the wide-angle X-ray diffraction region by an intense sharp reflection at 0.376 nm and further weaker reflections in the region corresponding to spacings of between 0.4–0.6 nm. No such structure was observed in our X-ray diffraction profiles. Secondly, at solvent concentrations between 2.4 and 9.0% (w/w), where inhomogeneity is believed to occur, almost the same phase transition sequence was recorded as that seen in the initial heating of the equilibrated samples. Thirdly, DSPE dispersed in glycerol concentrations greater than 24% (w/w) showed a different phase transition sequence during the first and second heating scans. Corresponding X-ray diffraction data for the small-and wide-angle scattering regions obtained during a heating scan of DSPE dispersed in 50% (w/w) glycerol is shown in Fig. 3. This shows a

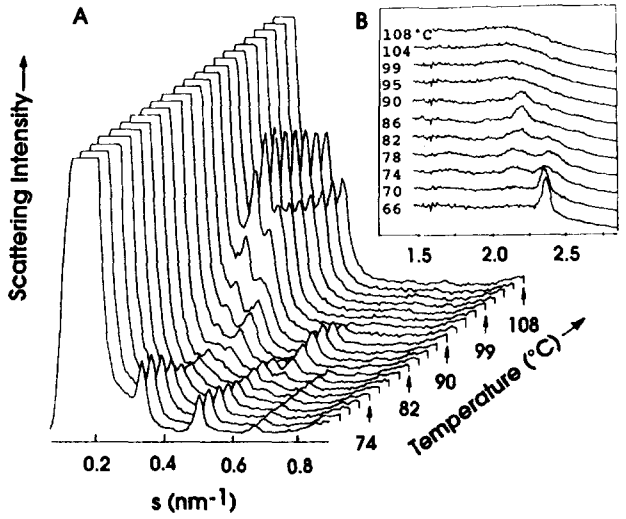

Fig. 3. Real-time X-ray diffraction patterns of distearoylphosphatidylethanolamine in glycerol (50%, w/w) showing the sequence of lamellar-gel to tilted lamellar crystalline to inverted hexagonal phase transitions. Data were acquired on the reheating at 5 C°/min the same sample shown in Fig. 2 immediately after cooling to 60° C. Each pattern represents scattering intensity accumulated during 24 s. (A) Small-angle scattering region; first order maxima are truncated to emphasize higher order diffractions; (B) corresponding wide-angle scattering intensity.

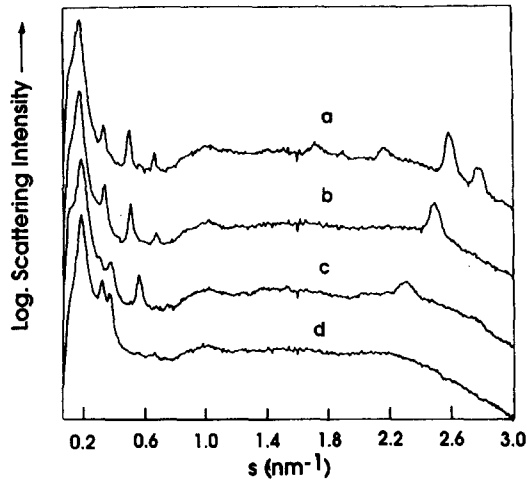

Fig. 4. Representative X-ray diffraction patterns obtained from a DSPE dispersion in 50% (w/w) glycerol of: a, L_c phase recorded at 65° C; b, L_{β} phase recorded at 65° C; c, $L_{c'}$ phase recorded at 86° C; d, H_{II} phase recorded at 108° C.

new lamellar phase, appearing at about 74° C, which coexists with, and progressively replaces an L_{β} phase with increasing temperature. During the slow process of replacement, an inverted hexagonal phase emerges at about 83° C. The wide-angle scattering pattern of the new lamellar phase (Fig. 3b) is characterized by a relatively strong reflection centred at 0.455 nm. This is assigned as a tilted crystalline phase $L_{c'}$ with possible triclinic acyl-chain packing [19]. Representative profiles for each of the four phases, L_c, $L_{c'}$, L_{β}, and H_{II}, are shown in Fig. 4 for comparison. Such an apparently abnormal phase transition sequence, from the metastable L_{β} to a more stable $L_{c'}$ phase, would be expected to be associated with release of heat. This has been confirmed in the corresponding thermal study (Fig. 1, right). Thermograms of DSPE dispersed in glycerol concentrations exceeding 24% (w/w) exhibited an exothermic event interposed between the two endothermic transitions. We assign the exotherm to a transition to $L_{c'}$. The gel to crystalline phase transition appears to be relatively slow at low temperatures and takes place through an annealing process which might be facilitated by a partial 'melting' of the lipid molecules (α phase). The two endotherms represent transitions L_{β}/α and $L_{c'}/H_{II}$, respectively.

The mechanism and kinetics of formation of lamellar crystalline phases from the lamellar gel phase was investigated by calorimetry. Differential scanning calorimetric curves obtained from a dispersion of DSPE in glycerol (85%, w/w) during heating from 60° C in the lamellar gel phase at different rates are shown in Fig. 5. The two-endotherm-one-exotherm pattern was observed at scanning rates of 5, 10, and 20 C°/min. Changes of the relative ratios of enthalpy of the two endotherms imply that the formation of the $L_{c'}$ phase is a relatively slow process even at elevated temperatures. Complete transition to the $L_{c'}$ phase

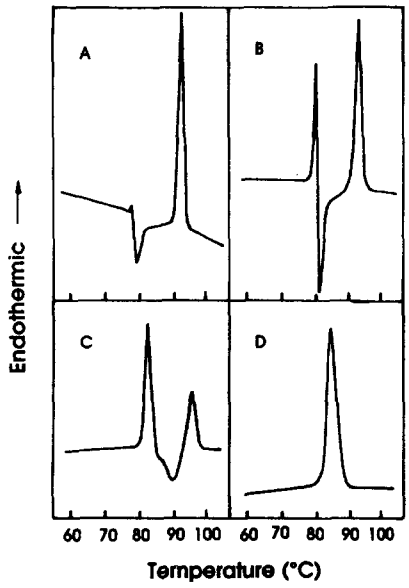

Fig. 5. DSC thermograms of a DSPE dispersion in glycerol (85%, w/w) with different heating rates. A, 5 C°/min; B, 10 C°/min; C, 20 C°/min, and D, 40 C°/min.

was achieved with a heating rate of 5 C°/min. At heating rate of 20 C°/min only partial transformation to the $L_{c'}$ phase was observed and at 40 C°/min there was an apparent transition directly from L_β to H_{II}.

Additional thermal studies to examine the formation of the crystalline phases are shown in Fig. 6. The same dispersion of DSPE in excess glycerol heated from 60° C in the lamellar gel phase at 5 C°/min was interrupted at temperatures below the onset of $L_\beta \rightarrow \alpha$ transition. Changes in enthalpy at constant temperature for different times before resuming heating were observed. The results, presented in Fig. 6, show that the rate of the exothermic transition increases with increasing temperatures. Thus the transit time at 75° C is about 6 min (Fig. 6C) and this decreases to about 2 min at a temperature 3° C higher (Fig. 6A). The thermal events recorded upon resumption of heating again exhibit a two-endotherm-one-exotherm pattern and we assign the transformation in this case as

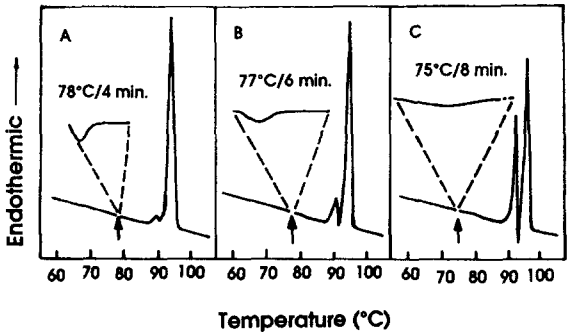

Fig. 6. DSC thermograms of a DSPE dispersion in glycerol (85%, w/w) at 5 C°/min. The heating program from 60° C to 110° C involves a pause at constant temperature: A, 78° C for 4 min; B, 77° C for 6 min; and C, 75° C for 8 min.

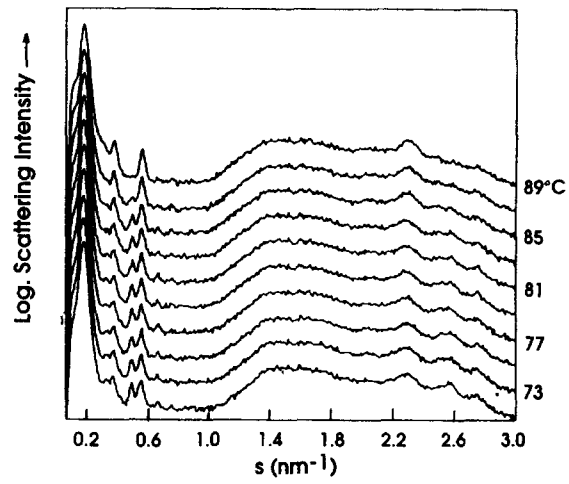

Fig. 7. Time-resolved X-ray diffraction profiles of DSPE/glycerol (24% w/w) showing the transition of one lamellar-crystalline structure (L_c) to another with tilted chains ($L_{c'}$).

$L_{c'} \rightarrow L_c \rightarrow H_{II}$. Taking into account the relative dimensions of the enthalpy changes the kinetics of transition from $L_{c'}$ to L_c phase shows increasing rates at higher temperatures. Thus conversion to L_c phase is almost complete when the temperature is held for 4 min at 78° C but when held for 8 min at 75° C the L_β phase converts predominantly to $L_{c'}$ phase.

The real-time X-ray diffraction data clearly demonstrate a direct transformation from L_c to H_{II} on the first heating of equilibrated dispersions of DSPE in glycerol (Fig. 2) and an $L_{c'}$ to H_{II} phase transition on reheating a sample cooled from the liquid-crystal state (Fig. 3). If a sample undergoing the transition $L_{c'} \rightarrow L_c$ on cooling or isothermal incubation is heated up from low temperatures, however, the phase transition sequence may be different. This point was examined by real-time X-ray scattering and the results are presented in Fig. 7. This shows that a dispersion of DSPE in 24% (w/w) glycerol is comprised of a mixture of two crystalline phases, L_c and $L_{c'}$, at about 70° C as indicated by their wide-angle diffraction patterns. An increase in temperature results in the gradual increase of the intensity of peaks corresponding to the $L_{c'}$ and a decease of scattering bands associated with the L_c phase until finally the $L_{c'}$ phase completely replaces the L_c at about 89° C. At higher temperatures there is an $L_{c'} \rightarrow H_{II}$ transition (not shown).

The dependence of repeat distances of different structures on the concentration of glycerol is summarized in Fig. 8. The dependence of repeat spacing on temperature for lamellar structures is relatively limited. It can be seen that the phase of DSPE-glycerol with the longest repeat spacing is the crystalline phase L_c. The crystalline phase, $L_{c'}$, characterised by acyl chains tilted with respect to the bilayer plane has an average repeat distance of about 90% of that of L_c phase. Assuming that the solvent layer in the crystalline phase is negligible, a tilting angle of about

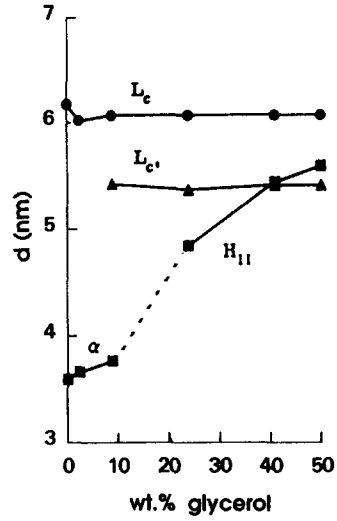

Fig. 8. Relationship between repeat spacing of different phases observed in DSPE and the concentration of glycerol in the mixture. Values of inverted hexagonal phase were obtained at 105° C. (For details see text.)

25.8° of the acyl chains in the $L_{c'}$ phase can be expected when calculated according to the method of Seddon et al. [20]. The repeat distance of lamellar-gel structure (not shown) is slightly less than that of lamellar-crystalline phase, but greater than that of tilted lamellar-crystalline structure. By contrast the repeat spacing of the nonlamellar structures, H_{II} or α at about 105° C, shows strong dependence on the glycerol content. The repeat spacing decreases with decreasing concentration of solvent until finally a less ordered structure forms. In the dry state, the repeat spacing is 3.7 nm. A similar relationship has been reported by Seddon et al. [17] in the diarachidoylphosphatidylethanolamine-water system where the dimensions of the H_{II} structure decrease with decreasing water content. A value of 3.7 nm for anhydrous phospholipid was obtained by extrapolation.

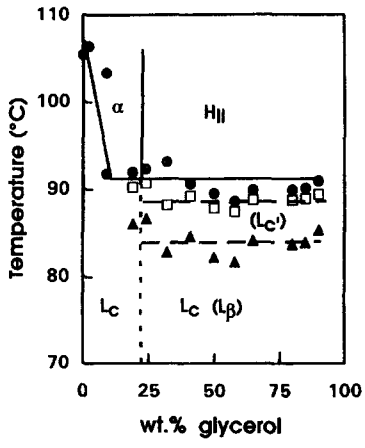

Fig. 9. Temperature-composition phase diagram of distearoylphosphatidylethanolamine in glycerol. Circles and solid line are transition from $L_c \rightarrow H_{II}$ upon initial heating; dashed lines and phase designation in brackets represent results of second heating; □, $L_{c'} \rightarrow H_{II}$; ▲, $L_\beta \rightarrow H_{II}$. α represents the imperfect form of H_{II} observed in limiting glycerol concentrations.

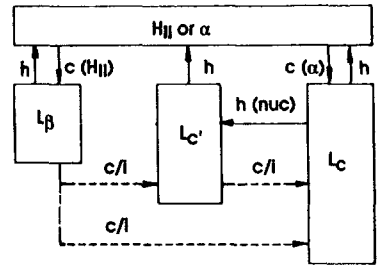

Fig. 10. Relationship between different phases of the DSPE/glycerol binary system. Solid arrows indicate observed transitions; dashed arrows represent possible to occur transitions that require prolonged incubation. L_c, $L_{c'}$, L_β, H_{II}, and α represent crystalline, tilted crystalline, gel, inverted hexagonal, and imperfect hexagonal phases, respectively. h, c, and c/i indicate the temperature treatment – heating, cooling, and cooling or isothermal incubation, respectively. h(nuc) is a heating process of L_c in the presence of $L_{c'}$.

Phase transition behaviour of DSPE/glycerol mixture during the first and second heating scans are summarized in a provisional binary phase diagram shown in Fig. 9. As the determination of onset temperatures of the phase transition during second heating is problematic, the values used are peak temperatures T_{max} from the thermograms presented in Fig. 1. The average transition temperatures for DSPE dispersions in glycerol concentrations greater than 24% (wt.) are: $L_c \rightarrow H_{II}$, 91° C; $L_\beta \rightarrow H_{II}$, 83° C; and $L_{c'} \rightarrow H_{II}$, 88° C. No lamellar liquid-crystal phase was detected in this study.

4. Discussion

4.1. Phase transition sequences and the relative stability of the two crystalline phases

Five different phases, L_c, $L_{c'}$, L_β, L_α, and H_{II}, have been reported in studies of different long-chain phosphatidylethanolamines in water [17,20,21]. The relative stabilities of the four lamellar phases have been categorized according to differences in the enthalpy values of transition between the respective phases [20]. It was concluded that the rank order of enthalpy was β_2 (designated as L_c in this work) < β_1 (equivalent to $L_{c'}$) < L_β < L_α.

The interrelationships between the different phases formed in the DSPE/glycerol binary system are presented in Fig. 10. No lamellar liquid-crystal phase was identified in the absence of water as clearly demonstrated by real-time X-ray diffraction profiles. This is due to a decrease in transition temperature towards the inverted hexagonal phase and an increase in transition temperature from the gel/subgel phase to the higher temperature phase [14] induced by glycerol. One explanation of this effect may be an enhancement of the interactions between adjacent lipid head groups in the presence of glycerol.

The abolition of the liquid-crystal phase by glycerol on the simple lipid system DSPE may have some biological implications. The effect of glycerol, for example, on lipid phase behaviour appears to be inconsistent with the liquid-crystal phase stabilization model in explaining the action of glycerol as a cryoprotectant. The relationship between its ability to promote non-bilayer structure and its role as a cryoprotectant can, however, be reconciled with the lipid phase separation model [2]. Another aspect that is emphasized by the data is that the role of water in preserving physiological functions cannot be entirely replaced by glycerol which does not favour the liquid-crystal state of biomembranes.

Of the three lamellar phases, L_c, $L_{c'}$, and L_β, L_c is the most stable. Once formed, the acyl chain packing arrangement will be preserved upon heating until the chains melt at high temperatures. The other two lamellar phases can transform directly to liquid-crystal phase (H_{II}) at fast heating rates. An example of this is shown in Fig. 5D in the case of L_β with a heating rate of 40 C°/min and in Fig. 1 and Fig. 3 for $L_{c'}$. A slower heating rate at 20 C°/min or less will cause the L_β to relax to $L_{c'}$ via an intermediate liquid-crystal phase. Several minutes incubation of the DSPE dispersion at around 75–78° C will result in the formation of L_c phase during either the incubation or further heating.

The apparently abnormal phase transition sequence of $L_\beta \rightarrow L_{c'}$ that occurs upon heating has already been reported [14]. According to the relaxation model developed by Tenchov [8], free energy changes of different phases along with temperature are presented in Fig. 11. As is shown, the transition temperature of $L_{c'} \rightarrow H_{II}$ is higher than that of $L_\beta \rightarrow H_{II}$. Thus the liquid-crystal phase between the two temperatures can be taken as metastable and may relax to the more stable $L_{c'}$ phase. Likewise, the liquid-crystal phase at temperatures between the transition temperature of $L_{c'} \rightarrow H_{II}$ and that of $L_c \rightarrow H_{II}$ is also metastable. This indicates the possible relaxation to L_c which, to our knowledge, was demonstrated the first time in the present study as shown in Fig. 6. Furthermore, the features of the temperature-dependent relaxations also implies that the formation of the $L_{c'}$ and L_c involves some kind of rearrangement of the head groups and/or acyl

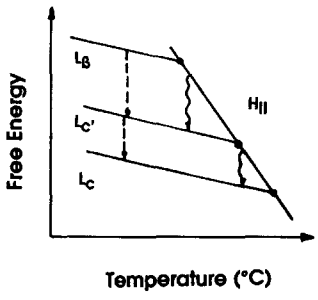

Fig. 11. Schematic illustration of the free energy changes of different phases vs. temperature. Wavy arrows indicate fast relaxations under defined conditions and dashed arrows represent slow relaxation processes.

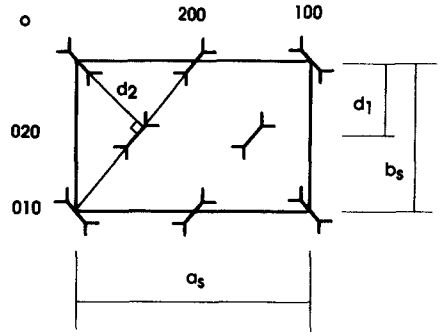

Fig. 12. Schematic presentation of the subcell of HS1 arrangement of acyl chains.

chains of the lipid molecules. Disordering of the hydrocarbon chains may enhance the relaxation process. At present, mechanisms concerning the transformations of $L_\beta \rightarrow L_{c'}/L_c$ and $L_{c'} \rightarrow L_c$ at low temperature are still unclear.

The high temperature phase is the regular H_{II} phase if the concentration of glycerol is greater than 24% (w/w). When solvent is limiting, the hexagonal phase appears to be somewhat irregular (denoted as α). The consequent phase sequence on cooling process is $H_{II} \rightarrow L_\beta$ in the former, and $\alpha \rightarrow L_c$ in the latter case.

4.2. Acyl chain arrangement in crystalline phase

The wide-angle diffraction pattern of the L_c phase in this study indicates that the acyl chains are packed in a hybrid orthorhombic arrangement, designated HS1 by Abrahamsson et al. [22]. It is analogous to the β_2 structure of dilauroylphosphatidylethanolamine [20]. Fig. 12 shows a cross-section of a subcell of the hydrocarbon chain arrangement. Although calculation of the dimensions, a_s and b_s, has been made by Ruocco and Shipley [23] according to Equation 1, the arbitrary assignment of d_1 and d_2 remains ambiguous as pointed out by Tenchov et al. [24].

$$a_s = 4d_1\tan\left(\sin^{-1}(d_2/2d_1)\right);\ b_s = 2d_1 \quad (1)$$

However, for those X-ray diffraction studies where more than two reflections of L_c are recorded, such ambiguity could be eliminated by trial and error. We found that by assigning the spacings of the first and second strongest reflections as d_2 and d_1, respectively, other diffractions can be fitted well into the subcell structure. Table 1 presents a summary of published data on subcell structural parameters. From the results the dimensions of the subcell can be described roughly as $a_s \approx 0.95$ nm and $b_s \approx 0.75$ nm. These provide a good agreement with that of the hybrid and simple orthorhombic subcells summarized by Abrahamsson et al. [22].

Another way to address the problem is to compare the specific density of HS1 subcell with that of the crystalline hydrocarbons. Using the L_c phase of DPPC as an example [24], where only two wide-angle X-ray diffractions were recorded, subcell parameters of $a_s = 1.070$ nm and $b_s =$

Table 1
Subcell structural parameters (nm) of lamellar crystalline phase (L_c)

lipid system	210	020	200		110		
	d_2	d_1	$a_s/2$	expt.	x	expt.	Ref.
DLPE/water	0.400	0.376	0.472	0.452	0.588	0.587	[20]
l-DPPE/aq. buffer	0.390	0.360	0.464	0.470	0.569	0.582	[21]
dl-DPPE/ibid	0.403	0.370	0.485	0.475	0.586	0.584	[21]
DSPE/glycerol	0.395	0.370	0.467	0.46	0.580	0.58	[14]
MGDG/water	0.414	0.379	0.494	–	0.601	0.59	[25]
DSPE/glycerol	0.407	0.381	0.481	0.480	0.598	0.597	*

Note: DLPE, DPPE, and DSPE, 1,2-dilauroyl-, dipalmitoyl-, and distearoylphosphatidylethanolamine; l and dl, l-enantiomer and racemic; aq. buffer, sodium borate buffer (50 mM, pH 8.0); MGDG, monogalactosyldiacylglycerol.
* This work.

0.774 nm can be derived in the same way as described for the phosphatidylethanolamine systems. Adopting the opposite approach the two parameters would have dimensions of 0.862 nm and 0.880 nm, respectively.

The length of the third side of the subcell, which includes two CH_2 groups, depends on the C-C bond length and the C-C-C bond angle. It is about 0.254 nm for a orthorhombic structure [22]. This is in good agreement with the value of 0.253 nm obtained from the bond angle and bond length of crystalline dimyristoylphosphatidic acid [26]. Using these parameters, the specific density in the acyl chain region can be calculated as 0.822 g cm^{-3} if values of $a_s = 1.070$ nm and $b_s = 0.774$ nm are used. The corresponding value of specific density is 0.898 g cm^{-3} if values of $a_s = 0.862$ nm and $b_s = 0.880$ nm are chosen. The specific densities of normal hydrocarbons range from 0.807 to 0.816 g cm^{-3} for hydrocarbons from n-octacosane to n-pentatriacontane. It is clear that subcell parameters of 1.070 nm and 0.774 nm provide a more reasonable agreement than the other assignment of a_s and b_s parameters. Thus the strongest diffraction in the L_c phase should represent the repeat distance of (210) plane as shown in Fig. 12. It should be emphasized that the precise assignment of phases and calculation of subcell parameters ultimately rely on accurate X-ray diffraction data.

Acknowledgements

Assistance of Wim Bras and staff of the Daresbury Laboratory was provided for real-time X-ray diffraction measurements. And Z.W.Y. is a scholarship holder under the Sino-British Friendship Scholarship Scheme.

References

[1] Lyman, G.H., Preisler, H.D. and Papahadjopoulos, D. (1976) Nature 262, 360–363.
[2] Quinn, P.J. (1985) Cryobiology 22, 456–60.
[3] Anchordoguy, T.J., Cecchini, C.A., Crowe, J.H. and Crowe, L.M. (1991) Cryobiology 28, 467–473.
[4] Crowe, J.H., Crowe, L.M., Carpenter, J.F. and Aurell Wistrom, C. (1987) Biochem. J. 242, 1–10.
[5] Crowe, J.H., Crowe, L.M., Carpenter, J.F., Rudolph, A.S., Aurell Wistrom, C., Spargo, B.J. and Anchordoguy, T.J. (1988) Biochim. Biophys. Acta 947, 367–384.
[6] Koynova, R.D., Tenchov, B.G. and Quinn, P.J. (1989) Biochim. Biophys. Acta 890, 377–380.
[7] Yu, Z.-W, Quinn, P.J. and Williams, W.P. (1994) Biochem. Soc. Tran. 22, 376.
[8] Tenchov, B. (1991) Chem. Phys. Lipids 57, 165–177.
[9] McDaniel, R.V., McIntosh, T.J. and Simon, S.A. (1983) Biochim. Biophys. Acta 731, 97–108.
[10] Simon, S.A. and McIntosh, T.J. (1984) Biochim. Biophys. Acta 773, 169–172.
[11] Tamura-Lis, W., Lis, L.J. and Quinn, P.J. (1987) J. Phys. Chem. 91, 4625–4627.
[12] Tamura-Lis, W., Lis, L.J. and Quinn, P.J. (1988) Biophys. J. 53, 489–492.
[13] O'Leary, T.J. and Levin, I.W. (1984) Biochim. Biophys. Acta 776, 185–189.
[14] Williams, W.P., Quinn, P.J., Tsonev, L.I. and Koynova, R.D. (1991) Biochim. Biophys. Acta 1062, 123–132.
[15] Lis, L.J. and Quinn, P.J. (1991) J. Appl. Cryst. 24, 48–60.
[16] Bun, C.W. and Howells, E.B. (1954) Nature (London) 174, 549–551.
[17] Seddon, J. M., Cevc, G., Kaye, R. D. and Marsh, D. (1984) Biochemistry 23, 2634–2644.
[18] Laggner, P. (1988) Topics Curr. Chem. 145, 173–202.
[19] Larsson, K. (1986) in The Lipid Handbook (Gunstone, F.D., Harwood, J.L. and Padley, F.B., eds.), Chapman and Hall.
[20] Seddon J.M., Harlos, K. and Marsh, D. (1983) J. Biol. Chem. 258, 3850–3854.
[21] Tenchov, B.G., Lis, L.J. and Quinn, P.J. (1988) Biochim. Biophys. Acta 942, 305–314.
[22] Abrahamsson, S., Dahlen, B., Lofgren, H. and Pascher, I. (1976) Prog. Chem. Fats Other Lipids 16, 125–143.
[23] Ruocco, M.J. and Shipley, G.G. (1982) Biochim. Biophys. Acta 691, 309–320.
[24] Tenchov, B.G., Lis, L.J. and Quinn, P.J. (1987) Biochim. Biophys. Acta 897, 143–151.
[25] Tsvetkova, N.M., Kapasi, M.F. and Quinn, P.J. (1993) Liquid Crystals 15, 65–74.
[26] Marsh, D. (1990) CRC Handbook of Lipid Bilayers, CRC Press.